Brain Connectivity

DOI: 10.1089/brain.2017.0536

Revisiting the functional and structural connectivity of large-scale cortical networks

Tien-Wen Lee[1,2,3]*, Shao-Wei Xue[1,2]

[1] Center for Cognition and Brain Disorders, Hangzhou Normal University, Hangzhou 311121, China

[2] Zhejiang Key Laboratory for Research in Assessment of Cognitive Impairments, Hangzhou 310015, China

[3] Department of Psychiatry, Dajia Lee's General Hospital, Lee's Medical Corporation, Taichung, Taiwan

* Corresponding author at: Center for Cognition and Brain Disorders, Hangzhou Normal University, Hangzhou, China

Address: Room 301, Shuyuan Building No. 19, Yuhangtang Rd No. 2318, Hangzhou 311121, Zhejiang Province, China

Email: dwlee_ibru@yahoo.com.tw

Tel: 86-15257152036

Fax: 86-571-28867717

Email addresses for other authors:
Shao-Wei Xue: xuedrm@126.com

Running Title: Functional and structural concordance of cortex

Keywords: Functional magnetic resonance imaging (fMRI); Diffusion weighted imaging (DWI); Diffusion tensor imaging (DTI); Resting fMRI (rfMRI); Functional connectivity; Structural Connectivity; Community detection

Brain Connectivity
Revisiting the functional and structural connectivity of large-scale cortical networks (DOI: 10.1089/brain.2017.0536)
This paper has been peer-reviewed and accepted for publication, but has yet to undergo copyediting and proof correction. The final published version may differ from this proof.

ABSTRACT

Multi-modal neuroimaging research has become increasingly popular, and structure-function correspondence is tacitly assumed. Researchers have not yet adequately assessed whether the functional connectivity (FC) and structural connectivity (SC) of large-scale cortical networks are in agreement. Structural magnetic resonance imaging (sMRI), resting-state functional MRI (rfMRI) and diffusion weighted imaging (DWI) datasets from 36 healthy subjects (age 27.4) were selected from a Rockland sample (Enhanced Nathan Kline Institute). The cerebral cortex was parcellated into 70 regions according to the Desikan-Killiany atlas for FC and SC analyses. Thresholded correlations in rfMRI and tractography derived from DWI were used to construct FC and SC maps, respectively. A community detection algorithm was applied to reveal the underlying organization, and modular consistency was quantified to bridge cross-modal comparisons. The distributions of correlation coefficients in FC and SC maps were significantly different. Approximately one-fourth of the connections in the SC map were located at a correlation level below 0.2 (d.f. 253). The index of modular consistency in the within-modality inter-individual condition (either FC or SC) was considerably greater than that in the between-modality intra-individual analogue. In addition, the SC-FC differential map (SC connections with lower correlations) revealed reliable modular structures. Based on these results, the hypothesized FC-SC agreement is partially valid. Contingent on extant neuroimaging tools and analytical conventions, the neural informatics of FC and SC should be regarded as complementary rather than concordant. Furthermore, the results verify the physiological significance of moderately (or mildly) correlated brain signals in rfMRI, which are often discarded by stringent thresholding.

Brain Connectivity
Revisiting the functional and structural connectivity of large-scale cortical networks (DOI: 10.1089/brain.2017.0536)
This paper has been peer-reviewed and accepted for publication, but has yet to undergo copyediting and proof correction. The final published version may differ from this proof.

Introduction

Complex network organization across different scales is one of the core features of the human brain. A network is defined by the interactive mechanisms between neural nodes. Network interaction is generally assessed by measuring functional connectivity (FC) and structural connectivity (SC). FC addresses the relationship of neural information shared, exchanged or integrated among neural nodes, whereas SC describes the hardwired architecture bridging different parts of a network. In neuroscience, function and structure correspondence is implicitly assumed but has not been adequately assessed on a large-scale level.

Neuroimaging research usually adopts two modalities of magnetic resonance imaging (MRI) to investigate the relationship between FC and SC, namely, functional MRI (fMRI) and diffusion weighted imaging (DWI). The blood oxygenation level-dependent (BOLD) signal measured by fMRI reflects regional blood flow and the degree of oxygen saturation, which is believed to be coupled to local neural activities. The strength of FC between two brain regions is frequently computed as a correlation coefficient of their BOLD fluctuations. Although located at a lower frequency range, BOLD dynamics are very informative, either in an activated or resting state (Biswal et al, 1995). DWI quantifies the anisotropic diffusion of water molecules along white matter (WM) tracts, which are converted to diffusion tensor imaging (DTI) for subsequent tractography. According to fMRI-DWI research, brain regions that are co-activated by visual stimuli exhibit WM connections (Phillips et al, 2012). A correspondence between FC and SC was also reported in a subset of default-mode network nodes, which are particularly active in the resting state (Greicius et al, 2009). Although previous empirical studies have investigated the relationship between inter-regional FC and SC, only a small number of them explored FC and SC relationships from a whole-brain perspective (Honey et al, 2009; Skudlarski et al, 2008). It is imperative to note that a substantial portion of multi-modal neuroimaging research skips the FC-SC concordance issue and adopts data fusion or data integration strategies to utilize the joint information provided by FC and SC (see (Sui et al, 2012) for an overview). Based on an implicit assumption of FC-SC concordance, several algorithms have been developed to integrate FC and SC (i.e., data integration). For example, functional coherence of the resting state fMRI (rfMRI) data was used to guide the clustering of white matter fibers (Lv et al,

Brain Connectivity
Revisiting the functional and structural connectivity of large-scale cortical networks (DOI: 10.1089/brain.2017.0536)
This paper has been peer-reviewed and accepted for publication, but has yet to undergo copyediting and proof correction. The final published version may differ from this proof.

2011), and conversely, DTI-derived SC was incorporated into a joint framework to determine FC (Bowman et al, 2012). In addition, "FC in SC" was regarded as a useful probe to detect changes in brain states (Li et al, 2013).

Despite these inspiring findings and optimism, several concerns regarding the FC-SC correspondence still remain. First, empirical results/conclusions obtained from regional analyses may not be appropriate for an extrapolation to the whole brain. Clarification of the commonality and uniqueness of FC and SC is a pre-requisite for physiological understanding of the joint FC-SC algorithms. Second, conventional FC analyses generally resort to correlation and subsequently use a stringent threshold to define significant connections – the FC map. Although the argument that a stronger neural interaction is accompanied by a higher correlation strength is persuasive, an intensely interacting network, in this case the brain, may show only moderate (or even mild) degrees of correlation because massive information computation and integration will result in a waveform change and phase delay in brain signals, hence reducing the degree of correlation (Chen et al, 2015; Grinband et al, 2008). Furthermore, extraordinarily high correlations are actually uncommon in biological systems that perform neuropsychological functions, which has been attributed to statistical issues (Kriegeskorte et al, 2009; Vul et al, 2009). This speculation led to a recent report, showing the presence of more than one FC map embedded in rfMRI data (Lee et al, 2014). In addition to the highly correlated FC neural pattern, other FC analogues exist that are characterized by lower correlation strengths. Thus, the connections in an SC map might include FCs with lower correlation levels that traditional methodologies discard. The direct consequence is a partial FC-SC mismatch, and the correspondence should not be taken for granted. Lastly, it has been proposed that the "information" provided by FC and SC is complimentary (Park and Friston, 2013). Empirical research has disclosed that the patterns of FC and SC may evolve with age in a partially dissociable way (Betzel et al, 2014), and the relationship between FC and SC may be decoupled in neuropsychiatric conditions (Michael et al, 2010; Skudlarski et al, 2010). These contradictory viewpoints regarding the FC-SC concordance issue demands empirical investigation to clarify.

This multi-modal neuroimaging study combined structural MRI (sMRI), rfMRI and DTI to perform a whole-brain survey of cortical connectivity. A modular analysis was applied to

Brain Connectivity
Revisiting the functional and structural connectivity of large-scale cortical networks (DOI: 10.1089/brain.2017.0536)
This paper has been peer-reviewed and accepted for publication, but has yet to undergo copyediting and proof correction. The final published version may differ from this proof.

elucidate the constituent neural communities. A community (or module) is described as a cluster of densely interconnected nodes that are sparsely connected with the rest of the network. The human cortex is always metabolically and electrically active, whether during purposeful behavior or during rest. The hybrid rfMRI and modular analyses enable the simultaneous assessment of several prominent neural networks/modules, including the default mode, sensorimotor, linguistic, visuo-associative, cognitive-executive, and temporal limbic networks, among others (Lee et al, 2014; Moussa et al, 2012; Xue et al, 2014). Notably, the modular organizations reported by different research groups are somewhat consistent. The consistency may originate from the small worldness property of the brain, which is robust to "structural decay" (Kaiser et al, 2007). In other words, although the connectivity patterns in either FC or SC become sparser with more stringent thresholds, the underlying modular structures remain. In addition, the similarity/dissimilarity of modular structures in FC and SC maps is quantifiable, which allows a direct cross-modal comparison of FC and SC. Accordingly, we chose community detection as the main surrogate to explore the FC-SC concordance issue. We postulated that the more dissimilar the modular organizations between the SC-map and FC-map, the more unlikely that these maps are concordant. This research aimed to re-examine the FC-SC agreement and to verify the proposal that connections at lower correlation levels are physiologically relevant to the concept of FC (Lee et al, 2014).

Materials and Methods

Subjects

Thirty-six healthy, right-handed subjects in adulthood (ages above 18 and below 50) were selected from the dataset of the 1,000 Functional Connectome Project (Rockland sample, Enhanced Nathan Kline Institute; NKI-RS), with a mean age of 27.4 years (19 – 42) and a balanced gender ratio. No significant difference in age was observed between genders. The data source used by this study met the criteria of “NKI-RS Neuroimaging Data Release” to maintain protection of participants' privacy.

Brain Connectivity
Revisiting the functional and structural connectivity of large-scale cortical networks (DOI: 10.1089/brain.2017.0536)
This paper has been peer-reviewed and accepted for publication, but has yet to undergo copyediting and proof correction. The final published version may differ from this proof.

MRI data acquisition and preprocessing

Four different image modalities were included in the analysis: T1-weighted sMRI, rfMRI, DWI and T2-weighted sMRI. All MRI images covered the whole brain and were acquired using 3.0 Tesla Siemens Magnetom Trio (a Tim system; Siemens Medical Solutions, Erlangen, Germany). The detailed scanning protocol can be accessed at the webpage http://fcon_1000.projects.nitrc.org/indi/pro/nki.html; the parameters are briefly summarized here. A high-resolution MPRAGE sagittal sMRI was used to facilitate the anatomical description and to register both functional and diffusion data (TR, 2,500 ms; TE, 3.1 ms; flip angle, 8°; FOV, 256x256 mm; slice thickness, 1.0 mm; voxel size, 1x1x1 mm^3; number of slices, 192). Sequential T2*-weighted transversal echoplanar images (EPIs) were recorded (TR, 2.5 s; TE, 30 ms; flip angle, 80°; FOV, 216x216 mm; slice thickness, 3.0 mm; voxel size, 3x3x3 mm^3; number of slices, 38) to trace dynamic changes in the resting-state BOLD signals. Two hundred and sixty whole-brain EPI images were collected for a period of 10 min and the first five EPI volumes were discarded to allow for signal equilibrium. Sixty-four direction DWI was acquired in the transverse orientation for fiber tracking (TR, 10.0 s; TE, 91 ms; FOV, 256x256 mm; slice-thickness, 2.0 mm; voxel size, 2x2x2 mm^3; number of slices, 58; b-value 1000s/mm^2; fat suppression).

The analytical platform FreeSurfer was applied to T1-weighted sMRI to segment gray matter and WM and was used to parcellate the cortical mantle into 70 neuroanatomical labels (Desikan-Killiany Atlas) (Dale et al, 1999; Desikan et al, 2006; Fischl et al, 1999). The result was examined by the associated software FreeView, and the observed topological or segmentation errors, if any, were in turn corrected by FreeSurfer (approximately 30 min of manual editing for each subject). Since the EPI signal in the orbitofrontal cortex is susceptible to artefacts (medial and lateral OFC in both hemispheres) and some regions are not pertinent to this research (i.e., "unknown" and a small bank at the superior temporal sulcus), these areas were not included in further analyses, resulting in 62 remaining regions of interest (ROIs); see Table 1 for details and abbreviations. These ROIs are the surrogate neural nodes used to explore FC and SC.

[Table 1 around here]

Brain Connectivity
Revisiting the functional and structural connectivity of large-scale cortical networks (DOI: 10.1089/brain.2017.0536)
This paper has been peer-reviewed and accepted for publication, but has yet to undergo copyediting and proof correction. The final published version may differ from this proof.

The Analysis of Functional NeuroImages software package (AFNI) was used to process the acquired EPI data (Cox, 1996). The analytic streamline developed by Jo et al. was adopted to prepare the rfMRI images (Jo et al, 2010; Lee et al, 2014; Xue et al, 2014). The preprocessing steps for the rfMRI data comprised despiking, slice-time correction, realignment (motion-corrected), registration to the T1 anatomy, spatial smoothing (6 mm), and bandpass filtering to 0.01–0.08 Hz (Biswal et al, 1995). Several regressors were created and modeled as nuisance variables, comprising twelve movement parameters (means and derivatives), third-order polynomials to fit the baseline drift, and tissue-based regressors of the WM (global and local) and ventricles (Jo et al, 2010) (two additional subjects were excluded due to excessive head movement greater than the width of one voxel). The tissue-based regressors were constructed with the help of the segmentation results obtained from FreeSurfer. Cross-talk between FreeSurfer and AFNI was achieved by SUMA (AFNI associated software). The whole-brain signal was not incorporated into the rfMRI regression model (Saad et al, 2012; Scholvinck et al, 2010). Cross-modal registration was achieved by non-linear warping using a weighted local Pearson correlation as a cost function (Saad et al, 2009).

DTI is derived from DWI and provides directional information for WM tract bundles. This research used the software TORTOISE (ver 2.5.1) to pre-process DWI for volume registration (motion correction), alignment to individual T1 sMRI data (mediated by the b0 volume), adjustment of the tensor vector, and correction for eddy currents and sequence-induced distortion (Pierpaoli et al, 2010). Conversion of DWI to DTI and subsequent tractography were accomplished using FATCAT (a set of AFNI-affiliated programs), which improves tractography by including diagonal tract propagation (probabilistic; default threshold of FA 0.2, minimum physical distance 20 mm, maximum angle 60°, and threshold fraction 0.01) (Taylor and Saad, 2013). Whole-brain probabilistic tractography was also performed and the quality of the tractography was visually checked by SUMA (Saad and Reynolds, 2012). Notably, FATCAT, SUMA, and the results of FreeSurfer are nicely integrated under the AFNI framework; thus, this platform is convenient for multi-modal analyses.

Brain Connectivity
Revisiting the functional and structural connectivity of large-scale cortical networks (DOI: 10.1089/brain.2017.0536)

FC and SC analyses

The averaged time course for each ROI was extracted, and a Pearson correlation coefficient was calculated that represented the connectivity strength for any pair of ROIs. Consequently, a 62x62 correlation matrix was generated for each subject. Since the FC connections among ROI pairs may be mediated by indirect connections and are not completely independent (62x61/2 = 1921), the false discovery rate (FDR) correction was applied to manage the multiple comparison issue. Rather than controlling the chance of any false positives (Bonferroni's correction of the two-tailed *P* value 0.05 would be $0.05/2/1921 = 1.3x10^{-5}$), FDR controls the expected proportion of false positives among supra-threshold connections. An FDR threshold is determined from the observed *P-value* distribution of Pearson's correlation coefficients and hence adapts to the data (Benjamini and Hochberg, 1995). In this study, FC was thresholded using a false discovery rate < 0.001, which was equivalent to a *P* value of 10^{-3} to 10^{-4} (varied among subjects). The FC map was binarized into values of one (connected) and zero (disconnected).

Given the small worldness property of brain networks, varying analytic parameters and thresholds may yield similar modular organizations. We therefore utilized community detection method to reveal the innate structure that underlies connectivity patterns and to facilitate subsequent FC and SC comparisons. The optimal algorithm for modularity analysis is still an open question (Bassett et al, 2011; Good et al, 2010). This research applied the recently released SurpriseMe algorithm to characterize the network community structure, which uses probability measures, rather than an artificial modularity index (Aldecoa and Marin, 2014). SurpriseMe calculates the global network parameter "Surprise", which is the unlikeliness of finding the observed number of intra-community links in a randomly connected network, to evaluate the quality of the network partition. In practical terms, Surprise is quantified based on a cumulative hypergeometric distribution, and its value is equal to the negative logarithm of the cumulative probability. The best partition of a network is determined by maximizing the Surprise value among seven state-of-the-art community-detection algorithms (Aldecoa and Marin, 2014).

Based on the results of individual FC analyses, group-level representative FC map was generated using a modified permutation test. The idea is simple and straightforward: we postulated that the connections in the individual FC map followed a random process. The

Brain Connectivity
Revisiting the functional and structural connectivity of large-scale cortical networks (DOI: 10.1089/brain.2017.0536)
This paper has been peer-reviewed and accepted for publication, but has yet to undergo copyediting and proof correction. The final published version may differ from this proof.

total number of significant connections for each subject was maintained and an artificial FC map was generated using random connections. The summation of 36 individual artificial maps (matrices) would result in a simulated "group score" matrix with a maximum value of 36 and a minimum value of 0 at each connection. Repeating the process 10,000 times would yield a distribution of group scores (0 to 36) at each connection. Then, compared with the true, observed group score matrix, we stipulated that the representative connections are the connections showing group scores greater than 99% of the 10,000 simulations (or $P < 0.01$). In other words, only consistent, across-subject connections survive this procedure, and these connections constitute the group-level FC map. The statistical significance of the derived group-level FC pattern was assessed using the following formula of binomial distribution with a degree of N: $P = \sum_{i=n}^{N} C(N,i) * p^i * q^{N-i}$, where N is the total number of possible connections, n is the observed number of connections, p is 0.01, q is 0.99 (1 minus p), and C(N,i) is the *ith* coefficient. When n approaches p*N, P is approximately 0.5. If significant values are simultaneously observed for many connections (p*N << n), the P value is expected to be very small, and the null hypothesis that the FC map is generated randomly will be rejected.

Similar to the FC analysis, individual SC results were binarized according to the presence or absence of connecting fiber bundles between any pair of ROIs, then subjected to community detection. A group-level SC map was obtained using a similar simulation process iterated 10,000 times. The mathematic software MATLAB was used to manage the above permutation processes and non-parametric statistical analyses (Mathworks, Natick, MA, USA). The modular structures of group-level FC and SC maps were also determined using SurpriseMe. The connections that were concordant between FC and SC maps are illustrated and discussed in **Supplementary Material** (Supp. Figures 3-6).

Comparison of FC and SC

A higher correlation in EPI signals between different brain regions has been suggested to implicate stronger neural interaction. Accordingly, correlation strengths are typically stringently thresholded to produce FC maps. Previous (regional) research has proposed

Brain Connectivity
Revisiting the functional and structural connectivity of large-scale cortical networks (DOI: 10.1089/brain.2017.0536)
This paper has been peer-reviewed and accepted for publication, but has yet to undergo copyediting and proof correction. The final published version may differ from this proof.

that SC is highly indicative of FC (Ansari et al, 2011; Greicius et al, 2009; Hagmann et al, 2008; Phillips et al, 2012; Teipel et al, 2010), implying that the connections in an SC map are associated with higher functional connectivity strengths. FC and SC were compared from three different perspectives to examine whole-brain SC-FC concordance/discordance and verify the assumption that lower correlations may still possess physiological importance (i.e., some connections in SC were indeed associated with lower FC): distribution, similarity, and the SC-FC differential map, as elaborated below.

The distributions of correlation coefficients in FC and SC maps were computed and compared. Specifically, the correlation coefficients of BOLD signals for the significant connections in the FC map constituted one set, and the correlation coefficients of BOLD signals for the connections defined by the presence of inter-regional fiber tracts in the SC map constituted another set. The two sets of correlation coefficients were compared using the Kolmogorov-Smirnov (KS) test. If the KS test failed to reach significance, then the SC connections were also located at a higher BOLD correlation level. The across-subject grand histograms of correlation coefficients in FC and SC were constructed for illustration.

The Jaccard index was used to summarize the similarity between the modular structures in FC and SC and further assess the correspondence of SC and FC (Steen et al, 2011). The formula of the metric is: $Jij = |Ai \cap Bj| / |Ai \cup Bj|$, where *A* and *B* are two different neural networks (i.e., SC or FC after thresholding). After partition, *Ai* is the set of nodes within a particular community *i* from network *A*, and *Bj* is the set of nodes within a particular community *j* from network *B*. Therefore, the total Jaccard index is $J = \sum_i \sum_j Jij$.

A nice feature of the Jaccard index is that arbitrary numbering of communities across partitions does not affect the result. The Jaccard index between FC and SC for each subject (N = 36) quantified the similarity in the within-subject between-modality condition (i.e., between rfMRI and DTI), whereas the Jaccard index between two different subjects' FC (or SC; N = 36x35/2) quantifies the similarity in the between-subject within-modality condition (i.e., either rfMRI or DTI). The significant differences in Jaccard indices were assessed using independent sample t-tests.

Since this study particularly focused on the SC connections with lower BOLD correlation strengths, an SC-FC differential map was constructed using the subset of

Brain Connectivity
Revisiting the functional and structural connectivity of large-scale cortical networks (DOI: 10.1089/brain.2017.0536)

connections in the SC map that do not appear in the FC map, and not vice versa. A permutation process was performed similar to the processes used in *FC and SC analysis* (with the same threshold *p* 0.01 and non-parametric procedure) to examine whether the differences in individual SC and FC maps showed reliable patterns at the group level. The modular organization of the SC-FC differential map was also calculated.

Results

Modular analyses of FC and SC

FC and SC connections occupied 26.3% and 15.7%, respectively, of all possible connections. The average modular numbers of individual FC and SC maps were 6.0 and 5.7 (bi-hemispheric homologous connection mediated by the corpus callosum was not counted as a single module). Group-level FC and SC maps were tested using a permutation processes, each with a *P* value less than 10^{-10}, indicating that consistent patterns of connection were observed across subjects. The modular structure of the group-level FC map was grossly concordant with previous reports (Lee et al, 2014; Moussa et al, 2012; Xue et al, 2014), including visuo-associative areas (3, 17, 34, and 48; 5, 7, 9, 10, 25, 36, 38, 40, 41, and 56), sensorimotor and acoustic regions (1, 13, 18, 20, 26, 27, 30, 31, 32, 44, 49, 51, 57, 58, 61, and 62), higher order motor/cognitive regions in the frontal lobe (14, 15, 16, 45, 46, and 47; 2, 23, 33, and 54), and default mode and midline structures (6, 8, 11, 19, 21, 22, 24, 37, 39, 42, 50, 52, 53, and 55). The bilateral frontal poles (28 and 59) and temporal poles (29 and 60) were ungrouped. The modular structure of the group-level SC map was somewhat different from that of the FC map, comprising visuo-associative areas and superior parietal region (3, 5, 7, 8, 9, 10, 12, 17, 21, 25, 34, 36, 38, 39, 40, 41, 43, 48, 52, and 56), limbic temporal region (4 and 29; 35 and 60), fronto-temporo-parietal network in the ventral brain (2, 6, 11, 14, 15, 16, 18, 20, 26, 27, 30, and 31; 33, 37, 42, 45, 46, 47, 49, 51, 57, 58, 61, and 62), and frontal and cingulate structures (1, 22, 23, 24, 28, 32, 53, 54, 55, and 59; 13, 19, 44, and 50). The numbers in the parentheses are area codes, please refer to Table 1. Figures 1 and 2 illustrate the group-level FC and SC maps and the corresponding modular structures visualized by BrainNet Viewer (http://www.nitrc.org/projects/bnv/). The Surprise values of group-level FC and SC maps were 139.2 and 142.2 (both with a binomial distribution $P < 10^{-10}$), respectively.

[Figures 1 and 2 around here]

Brain Connectivity
Revisiting the functional and structural connectivity of large-scale cortical networks (DOI: 10.1089/brain.2017.0536)
This paper has been peer-reviewed and accepted for publication, but has yet to undergo copyediting and proof correction. The final published version may differ from this proof.

FC and SC comparisons

This study designed three complementary analyses to compare FC and SC maps. The distributions of correlation coefficients were examined using the KS test. For each subject, the statistics differed at the level of $P < 10^{-10}$, with a mean KS of 0.34 (SD 0.12) for the thresholded FC distribution and a mean KS 0.18 (SD 0.04) for the full (unthresholded) FC distribution. A grand histogram of all the individual data revealed that the connections in the SC map actually contain connections with lower correlation strength in BOLD dynamics, see Figure 3. Since FC is thresholded using stringent criteria, the histogram was short on one tail. Approximately one-fourth of the SC connections were estimated to be associated with correlation coefficients (in FC) of less than 0.2. Because the number of connections in the FC map was approximately 1.7 times greater than that in the SC map and the FC map was generated using thresholding, some connections with a high correlation level in the FC map were absent in the SC map (data not shown), consistent with a previous report (Honey et al, 2009).

The modular consistency, as reflected by the Jaccard index, in within-modality between-subject conditions (SC: mean 0.36, SD 0.12; FC: mean 0.26, SD 0.08) is significantly larger than the cross-modality within-subject analogue (mean 0.17, SD 0.03), both with $P < 10^{-10}$. The modular consistency analysis implied a significant difference in the topology of FC and SC maps. (Note: different sampling strategies were adopted to explore this issue, and the conclusion still holds; see the **Supplemental Data** for details).

Based on the two positive findings described above, a group-level SC-FC differential map was constructed ($P < 10^{-10}$) and its constituent neural communities were detected (Surprise value 58.4), including visuo-associative areas and parietal regions (3, 4, 5, 6, 7, 8, 9, 10, 17, 18, 20, 21, 25, 31, 34, 35, 36, 37, 38, 39, 40, 41, 48, 49, 51, 52, 56, and 62), inferior frontal gyrus (15, 16, 46, and 47), temporal sub-regions (11, 29, 42, and 60), midline structures (1, 13, 19, 32, 44, and 45), and sub-networks in the frontal lobe (14, 24, 45, and 55; 2, 23, 28, 33, 54, and 59; 26, 30, 57, and 61); see Figure 4. The bilateral rostral anterior cingulate (22 and 53), supramarginal gyri (27 and 58) and parahippocampus (12

and 43) remained ungrouped. Note that the SC-FC differential map reflects the SC connections at a lower correlation level, i.e., weaker FC.

[Figures 3 and 4 around here]

Discussion

The structure of the central nervous system is believed to underlie its function; therefore, FC and SC must have a correspondence across different neural network scales. At a large-scale brain network level, preliminary reports seemed to echo this viewpoint, and computational models were developed to explore FC that is informed by SC, and vice versa (Bowman et al, 2012; Greicius et al, 2009; Lv et al, 2011; Phillips et al, 2012; Skudlarski et al, 2008). However, researchers have not clearly determined whether extant neuroimaging equipment and analytical conventions are suitable to reveal the FC-SC relationship. This multi-modal research combined sMRI, rfMRI and DTI to construct FC and SC maps. Respective modular structures were retrieved and compared to examine their similarity/dissimilarity. The results challenge the assumption of FC-SC agreement.

Histograms of correlation coefficients in FC and SC maps revealed interesting insights to the issue of SC-FC concordance (Figure 3). Most previous empirical studies that compared SC and FC from pre-selected ROIs addressed the SC-FC correspondence and suggested that the connections in the SC map would possess a higher functional connectivity strength (Ansari et al, 2011; Greicius et al, 2009; Phillips et al, 2012; Teipel et al, 2010). This study examined whether the conclusion obtained from the regional analyses is applicable to the whole brain. If the SC map is an approximate representation of the FC map, their respective histograms should look similar, and the KS-test would be insignificant. This null hypothesis was rejected. Notably, approximately one-fourth of the SC connections displayed BOLD correlation levels less than 0.2 (d.f. 253), where no connections were present in the thresholded FC map. In addition, the shapes of the two histograms differed conspicuously (flatter for the SC map). Because SC provides hardwired connections that enable neural interactions, the results support the hypothesis that moderately (and even mildly) correlated connections in FC maps may still be pertinent to neural interactions (Lee et al, 2014). This conclusion is not surprising since the conditions

Brain Connectivity
Revisiting the functional and structural connectivity of large-scale cortical networks (DOI: 10.1089/brain.2017.0536)
This paper has been peer-reviewed and accepted for publication, but has yet to undergo copyediting and proof correction. The final published version may differ from this proof.

Brain Connectivity
Revisiting the functional and structural connectivity of large-scale cortical networks (DOI: 10.1089/brain.2017.0536)
This paper has been peer-reviewed and accepted for publication, but has yet to undergo copyediting and proof correction. The final published version may differ from this proof.

of a moderate degree of correlation are much more frequent than extremely high correlations in various psycho-physiological repertoires (Vul et al, 2009). Current FC approaches that preserve only the strongly correlated connections may lose information required for a holistic understanding of the resting-state brain.

Regarding multi-modal neuroimaging research, a critical consideration is the method used to design a cross-modal comparison. A previous report attempted to generate artificial rfMRI signals from an SC-informed computational model, and then compared the artificial FC with the observed FC (Honey et al, 2009). Briefly, the computational model simulated neuronal population dynamics, in which SC provided edge information between neural nodes. In contrast to indirect inference via neuronal model simulation, this study committed to the data and used a community detection to enable direct comparison of FC and SC. A welcome feature of the modular analysis of the brain lies in its robustness to "structural decay" (Kaiser et al, 2007). In other words, although the FC-map is corroded by stringent thresholding and the fiber tracking algorithm may be inadequate to delineate complete structural connections, the underlying modular structures might still be retained. The Jaccard index has been applied to measure modular consistency in cross-modal and within-modal conditions (Moussa et al, 2012; Steen et al, 2011). It is interesting to note that the Jaccard index for the between-subject within-modality condition (either FC or SC) was significantly higher than its within-subject cross-modality counterpart. Specifically, the dissimilarity of the modular organization between the SC and FC maps for the same subject was considerably greater than the modular organization of the FC map (and SC map) across different subjects. Thus, the hypothesis of intra-individual FC-SC concordance was not supported. Other potential causes that may affect the results should also be considered, such as different scanning parameters and analytic methods. Although not the main focus of this research, our analysis replicated a finding from a previous systemic survey that FC connections with a high correlation level may have no SC connections (Honey et al, 2009), adding another piece of evidence refuting the assumption of perfect SC-FC concordance.

The global metabolic rate in the resting-state brain is similar to the rate observed when subjects performed psychological tasks (Gusnard and Raichle, 2001), implying that the brain still functions during relaxation. Consistent with this finding, rfMRI dynamics contain several active and synchronized modules, which are reproduced in the modular

Brain Connectivity
Revisiting the functional and structural connectivity of large-scale cortical networks (DOI: 10.1089/brain.2017.0536)
This paper has been peer-reviewed and accepted for publication, but has yet to undergo copyediting and proof correction. The final published version may differ from this proof.

analysis of the group-level FC map (Lee et al, 2014; Moussa et al, 2012; Xue et al, 2014). The modular structures of FC and SC maps are somewhat different. The SC modules seem to respect lobar anatomy and the hardwired organization of WM bundles, whereas FC modules, as shown in our results and in previous studies, reflect emergent synchronization of function-pertinent networks that may involve distant neural nodes. In detail, the SC modules are categorized into two different classes. The first class is largely mediated by regional cortico-cortical association fibers, including the visuo-associative network in posterior brain regions (parietal and temporal areas could be directly connected by vertical occipital fasciculi), frontal and cingulate network, and temporal network (Schmahmann et al, 2008). In contrast to the "local property" of the first class of SC modules, the second counterpart encompasses broad areas in the ventral brain (frontal, temporal and inferior parietal regions), which may be linked by inferior longitudinal, inferior occipito-frontal, and uncinate fasciculi.

Based on the partial disagreement of SC and FC maps, a permutation process was applied to create an SC-FC differential map, which was equivalent to the connections in the SC map with low correlation strength in the FC map. Robust statistics of the SC-FC differential map and significant Surprise values again rejected SC-FC concordance, yielding prominent and consistent (across subjects) modules such as the visuo-associative network, midline structures, and several sub-networks in frontal and temporal regions. The visuo-associative module in the SC-FC differential map is particularly intriguing since it bridges the primary visual cortex, ventral pathway, dorsal pathway, posterior midline structures, and attention network at a lower FC strength. The neural informatics of these areas are diverse and hence their correlation is not expected to be high; however, their integration is mandatory for proper visual functions. This finding resonates with the claim that connections with moderate or even mild correlation strengths may still be physiologically relevant. The modular results at different correlation strengths and from different imaging modalities imply that the network organization of the brain depends on the vantage point and does not obey a fixed partition.

Correspondence between the structure and function of the brain is tacitly assumed; furthermore, structure may underlie function. In the history of neuroscience, this viewpoint is traced back to the classical work on neurons by Remon Y Cajal (and many

Brain Connectivity
Revisiting the functional and structural connectivity of large-scale cortical networks (DOI: 10.1089/brain.2017.0536)
This paper has been peer-reviewed and accepted for publication, but has yet to undergo copyediting and proof correction. The final published version may differ from this proof.

others) (Sotelo, 2003), and has gained support from the neuronal level to the neural tissue level (Wang, 2010). This correspondence is also a belief that originates from materialism. Not surprisingly, recent multi-modal neuroimaging research has attempted to discover the agreement of FC and SC, and not vice versa (Honey et al, 2009; Lv et al, 2011; Phillips et al, 2012; Skudlarski et al, 2008). Although the present study highlights certain discrepancies between FC and SC, the results should not be viewed as evidence opposing the "doctrine of structure-function correspondence". The revealed FC-SC mismatch may originate from two sources. First, the selected definition of FC may bias the understanding of the whole picture of large-scale brain networks. The use of a strong correlation strength as a surrogate for FC is reasonable and appropriate; however, it inevitably will discard physiologically pertinent information at lower correlation strengths, which might host sub-networks characterized by massive information exchange, calculation, or integration. Second, modern neuroimaging tools *per se* may not be sufficiently competent to describe the entire picture of FC and SC, and various kinds of noise in fMRI and DWI/DTI may also contribute to the FC-SC discordance (Thomas et al, 2014). Complete FC-SC agreement is conceptually and ideally possible, but may not be achieved without referring to infrastructures at finer scales, i.e., the organization and physiological properties of neuronal tissues. Together, the information provided by rfMRI and DTI is more complementary than concordant (or redundant). The present study does not suggest that all mildly correlated connections are physiologically meaningful, and it is also worthwhile to replicate the analysis in an entirely independent dataset.

Conclusions

This study combined rfMRI, sMRI and DWI to examine the agreement of FC and SC and to investigate the claim that neural interactions with lower correlation levels may still be important. An AFNI framework was applied to facilitate multi-modal imaging processing, and a community detection algorithm was used to enable FC and SC comparisons. Modular analysis was adopted due to its tolerance of perturbations in connections. The results consistently disclosed FC-SC discrepancies from different perspectives, and verified the physiological significance of moderately (or mildly) correlated brain signals. This and previous studies also observed that a high correlation in FC may not be associated with

hardwired cortical connection, which may be mediated by indirect connection and/or subcortical synchronization (Honey et al, 2009). Accordingly, the neural informatics of FC and SC should be regarded complementary rather than concordant, and the validity of using one to inform the other is questionable. Furthermore, the conventional strategy used to analyze FC may be innately biased (toward a highly correlated regime) and may sacrifice some of the richness of brain dynamics.

Acknowledgement

This work was supported by Dajia Lee's General Hospital, Lee's Medical Corporation, Taichung, Taiwan.

Financial support

Natural Science Foundation of Zhejiang Province Grant LY17H180007; Social Development Project of Hangzhou 20170533B06.

Declaration of conflict of interest

No

Brain Connectivity
Revisiting the functional and structural connectivity of large-scale cortical networks (DOI: 10.1089/brain.2017.0536)
This paper has been peer-reviewed and accepted for publication, but has yet to undergo copyediting and proof correction. The final published version may differ from this proof.

Brain Connectivity
Revisiting the functional and structural connectivity of large-scale cortical networks (DOI: 10.1089/brain.2017.0536)
This paper has been peer-reviewed and accepted for publication, but has yet to undergo copyediting and proof correction. The final published version may differ from this proof.

References

Aldecoa R, Marin I. 2014. SurpriseMe: an integrated tool for network community structure characterization using Surprise maximization. Bioinformatics 30:1041-1042.

Ansari AH, Oghabian MA, Hossein-Zadeh GA. 2011. Assessment of functional and structural connectivity between motor cortex and thalamus using fMRI and DWI. Conf Proc IEEE Eng Med Biol Soc 2011:5056-5059.

Bassett DS, Wymbs NF, Porter MA, Mucha PJ, Carlson JM, Grafton ST. 2011. Dynamic reconfiguration of human brain networks during learning. Proc Natl Acad Sci U S A 108:7641-7646.

Benjamini Y, Hochberg Y. 1995. Controlling the false discovery rate: a practical and powerful approach to multiple testing. Journal of the royal statistical society Series B (Methodological):289-300.

Betzel RF, Byrge L, He Y, Goni J, Zuo XN, Sporns O. 2014. Changes in structural and functional connectivity among resting-state networks across the human lifespan. Neuroimage 102 Pt 2:345-357.

Biswal B, Yetkin FZ, Haughton VM, Hyde JS. 1995. Functional connectivity in the motor cortex of resting human brain using echo-planar MRI. Magn Reson Med 34:537-541.

Bowman FD, Zhang L, Derado G, Chen S. 2012. Determining functional connectivity using fMRI data with diffusion-based anatomical weighting. Neuroimage 62:1769-1779.

Chen G, Saad ZS, Adleman NE, Leibenluft E, Cox RW. 2015. Detecting the subtle shape differences in hemodynamic responses at the group level. Front Neurosci 9:375.

Cox RW. 1996. AFNI: software for analysis and visualization of functional magnetic resonance neuroimages. Comput Biomed Res 29:162-173.

Dale AM, Fischl B, Sereno MI. 1999. Cortical surface-based analysis. I. Segmentation and surface reconstruction. Neuroimage 9:179-194.

Brain Connectivity
Revisiting the functional and structural connectivity of large-scale cortical networks (DOI: 10.1089/brain.2017.0536)

Desikan RS, Segonne F, Fischl B, Quinn BT, Dickerson BC, Blacker D et al. 2006. An automated labeling system for subdividing the human cerebral cortex on MRI scans into gyral based regions of interest. Neuroimage 31:968-980.

Fischl B, Sereno MI, Dale AM. 1999. Cortical surface-based analysis. II: Inflation, flattening, and a surface-based coordinate system. Neuroimage 9:195-207.

Good BH, de Montjoye YA, Clauset A. 2010. Performance of modularity maximization in practical contexts. Phys Rev E Stat Nonlin Soft Matter Phys 81:046106.

Greicius MD, Supekar K, Menon V, Dougherty RF. 2009. Resting-state functional connectivity reflects structural connectivity in the default mode network. Cereb Cortex 19:72-78.

Grinband J, Wager TD, Lindquist M, Ferrera VP, Hirsch J. 2008. Detection of time-varying signals in event-related fMRI designs. Neuroimage 43:509-520.

Gusnard DA, Raichle ME. 2001. Searching for a baseline: functional imaging and the resting human brain. Nat Rev Neurosci 2:685-694.

Hagmann P, Cammoun L, Gigandet X, Meuli R, Honey CJ, Wedeen VJ, Sporns O. 2008. Mapping the structural core of human cerebral cortex. PLoS Biol 6:e159.

Honey CJ, Sporns O, Cammoun L, Gigandet X, Thiran JP, Meuli R, Hagmann P. 2009. Predicting human resting-state functional connectivity from structural connectivity. Proc Natl Acad Sci U S A 106:2035-2040.

Jo HJ, Saad ZS, Simmons WK, Milbury LA, Cox RW. 2010. Mapping sources of correlation in resting state FMRI, with artifact detection and removal. Neuroimage 52:571-582.

Kaiser M, Martin R, Andras P, Young MP. 2007. Simulation of robustness against lesions of cortical networks. Eur J Neurosci 25:3185-3192.

Kriegeskorte N, Simmons WK, Bellgowan PS, Baker CI. 2009. Circular analysis in systems neuroscience: the dangers of double dipping. Nat Neurosci 12:535-540.

Lee TW, Northoff G, Wu YT. 2014. Resting network is composed of more than one neural pattern: An fMRI study. Neuroscience 274:198-208.

Li X, Lim C, Li K, Guo L, Liu T. 2013. Detecting brain state changes via fiber-centered functional connectivity analysis. Neuroinformatics 11:193-210.

Lv J, Guo L, Li K, Hu X, Zhu D, Han J, Liu T. 2011. Activated fibers: fiber-centered activation detection in task-based FMRI. Inf Process Med Imaging 22:574-587.

Michael AM, Baum SA, White T, Demirci O, Andreasen NC, Segall JM et al. 2010. Does function follow form?: methods to fuse structural and functional brain images show decreased linkage in schizophrenia. Neuroimage 49:2626-2637.

Moussa MN, Steen MR, Laurienti PJ, Hayasaka S. 2012. Consistency of network modules in resting-state FMRI connectome data. PLoS One 7:e44428.

Park HJ, Friston K. 2013. Structural and functional brain networks: from connections to cognition. Science 342:1238411.

Phillips JS, Greenberg AS, Pyles JA, Pathak SK, Behrmann M, Schneider W, Tarr MJ. 2012. Co-analysis of brain structure and function using fMRI and diffusion-weighted imaging. J Vis Exp.

Pierpaoli C, Walker L, Irfanoglu M, Barnett A, Basser P, Chang L et al. 2010. TORTOISE: an integrated software package for processing of diffusion MRI data. Book TORTOISE: an Integrated Software Package for Processing of Diffusion MRI Data (Editor ed^ eds) 18:1597.

Saad ZS, Glen DR, Chen G, Beauchamp MS, Desai R, Cox RW. 2009. A new method for improving functional-to-structural MRI alignment using local Pearson correlation. Neuroimage 44:839-848.

Saad ZS, Gotts SJ, Murphy K, Chen G, Jo HJ, Martin A, Cox RW. 2012. Trouble at rest: how correlation patterns and group differences become distorted after global signal regression. Brain Connect 2:25-32.

Brain Connectivity
Revisiting the functional and structural connectivity of large-scale cortical networks (DOI: 10.1089/brain.2017.0536)
This paper has been peer-reviewed and accepted for publication, but has yet to undergo copyediting and proof correction. The final published version may differ from this proof.

Brain Connectivity
Revisiting the functional and structural connectivity of large-scale cortical networks (DOI: 10.1089/brain.2017.0536)
This paper has been peer-reviewed and accepted for publication, but has yet to undergo copyediting and proof correction. The final published version may differ from this proof.

Saad ZS, Reynolds RC. 2012. SUMA. Neuroimage 62:768-773.

Schmahmann JD, Smith EE, Eichler FS, Filley CM. 2008. Cerebral white matter: neuroanatomy, clinical neurology, and neurobehavioral correlates. Ann N Y Acad Sci 1142:266-309.

Scholvinck ML, Maier A, Ye FQ, Duyn JH, Leopold DA. 2010. Neural basis of global resting-state fMRI activity. Proc Natl Acad Sci U S A 107:10238-10243.

Skudlarski P, Jagannathan K, Anderson K, Stevens MC, Calhoun VD, Skudlarska BA, Pearlson G. 2010. Brain connectivity is not only lower but different in schizophrenia: a combined anatomical and functional approach. Biol Psychiatry 68:61-69.

Skudlarski P, Jagannathan K, Calhoun VD, Hampson M, Skudlarska BA, Pearlson G. 2008. Measuring brain connectivity: diffusion tensor imaging validates resting state temporal correlations. Neuroimage 43:554-561.

Sotelo C. 2003. Viewing the brain through the master hand of Ramon y Cajal. Nat Rev Neurosci 4:71-77.

Steen M, Hayasaka S, Joyce K, Laurienti P. 2011. Assessing the consistency of community structure in complex networks. Phys Rev E Stat Nonlin Soft Matter Phys 84:016111.

Sui J, Adali T, Yu Q, Chen J, Calhoun VD. 2012. A review of multivariate methods for multimodal fusion of brain imaging data. J Neurosci Methods 204:68-81.

Taylor PA, Saad ZS. 2013. FATCAT: (an efficient) Functional and Tractographic Connectivity Analysis Toolbox. Brain Connect 3:523-535.

Teipel SJ, Bokde AL, Meindl T, Amaro E, Jr., Soldner J, Reiser MF et al. 2010. White matter microstructure underlying default mode network connectivity in the human brain. Neuroimage 49:2021-2032.

Thomas C, Ye FQ, Irfanoglu MO, Modi P, Saleem KS, Leopold DA, Pierpaoli C. 2014. Anatomical accuracy of brain connections derived from diffusion MRI tractography is inherently limited. Proc Natl Acad Sci U S A 111:16574-16579.

Vul E, Harris C, Winkielman P, Pashler H. 2009. Puzzlingly high correlations in fMRI studies of emotion, personality, and social cognition. Perspectives on psychological science 4:274-290.

Wang XJ. 2010. Neurophysiological and computational principles of cortical rhythms in cognition. Physiological reviews 90:1195-1268.

Xue SW, Li D, Weng XC, Northoff G, Li DW. 2014. Different neural manifestations of two slow frequency bands in resting functional magnetic resonance imaging: a systemic survey at regional, interregional, and network levels. Brain Connect 4:242-255.

Brain Connectivity
Revisiting the functional and structural connectivity of large-scale cortical networks (DOI: 10.1089/brain.2017.0536)
This paper has been peer-reviewed and accepted for publication, but has yet to undergo copyediting and proof correction. The final published version may differ from this proof.

Table 1

Parcellation of 62 cortical brain regions and their abbreviations based on FreeSurfer atlas (odd number: left; even number: right).

#	Regions	Abbr.	#	Regions	Abbr.
1, 32	Caudal anterior cingulate cortex	cACC CAL	17, 48	Pericalcarine	
2, 33	Caudal middle frontal cortex	cMFC	18, 49	Postcentral gyrus	PoCG
3, 34	Cuneus	CUN			
19, 50	Posterior cingulate cortex	PCC			
4. 35	Entorhinal cortex	EC	20, 51	Precentral gyrus	PreCG
5, 36	Fusiform gyrus	FG			
21, 52	Precuneus	PCUN			
6, 37	Inferior parietal lobule	IPL			
22, 53	Rostral anterior cingulate	rACC			
7, 38	Inferior temporal gyrus	ITG			
23, 54	Rostral middle frontal cortex	rMFC			
8, 39	Isthmus cingulate gyrus	ICG			
24, 55	Superior frontal cortex	SFC			
9, 40	Lateral occipital complex	LOC	25, 56	Superior parietal lobule	SPL

Brain Connectivity
Revisiting the functional and structural connectivity of large-scale cortical networks (DOI: 10.1089/brain.2017.0536)
This paper has been peer-reviewed and accepted for publication, but has yet to undergo copyediting and proof correction. The final published version may differ from this proof.

Brain Connectivity
Revisiting the functional and structural connectivity of large-scale cortical networks (DOI: 10.1089/brain.2017.0536)

10, 41	Lingual gyrus	LG		26, 57	
	Superior temporal gyrus	STG			
11, 42	Middle temporal gyrus	MTG		27, 58	
	Supramarginal gyrus	SMG			
12, 43	Parahippocampal gyrus	PHG		28, 59	Frontal pole
		FP			
13, 44	Paracentral lobule	PCL		29, 60	
	Temporal pole	TP			
14, 45	Inferior frontal gyrus (opercular)	IFGope		30, 61	Transverse temporal gyrus
		TTG			
15, 46	Inferior frontal gyrus (orbital)	IFGori		31, 62	Insula
		INS			
16, 47	Inferior frontal gyrus (triangular)	IFGtri			

Figure Legends

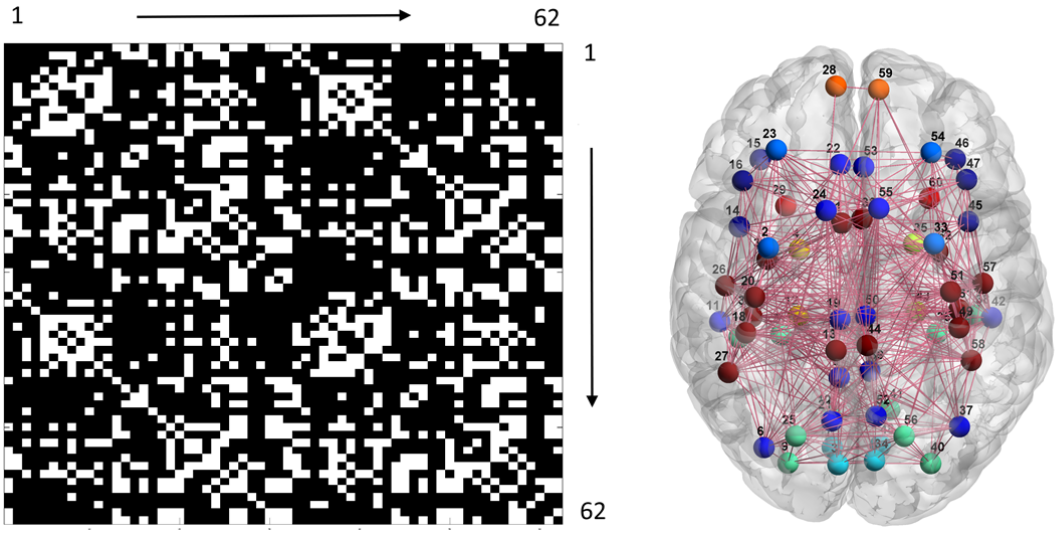

Fig. 1. Left: group-level FC map (62x62 matrix). White and black indicate the presence and absence of connections. The numbers along the border of the matrix stand for the area codes (see Table 1). Right: results of the associated community detection analysis. Filled circles and solid lines respectively represent neural nodes (ROIs) and connections. Different modules are highlighted by different colors, and the numbers are the area codes.

Brain Connectivity
Revisiting the functional and structural connectivity of large-scale cortical networks (DOI: 10.1089/brain.2017.0536)
This paper has been peer-reviewed and accepted for publication, but has yet to undergo copyediting and proof correction. The final published version may differ from this proof.

Brain Connectivity
Revisiting the functional and structural connectivity of large-scale cortical networks (DOI: 10.1089/brain.2017.0536)

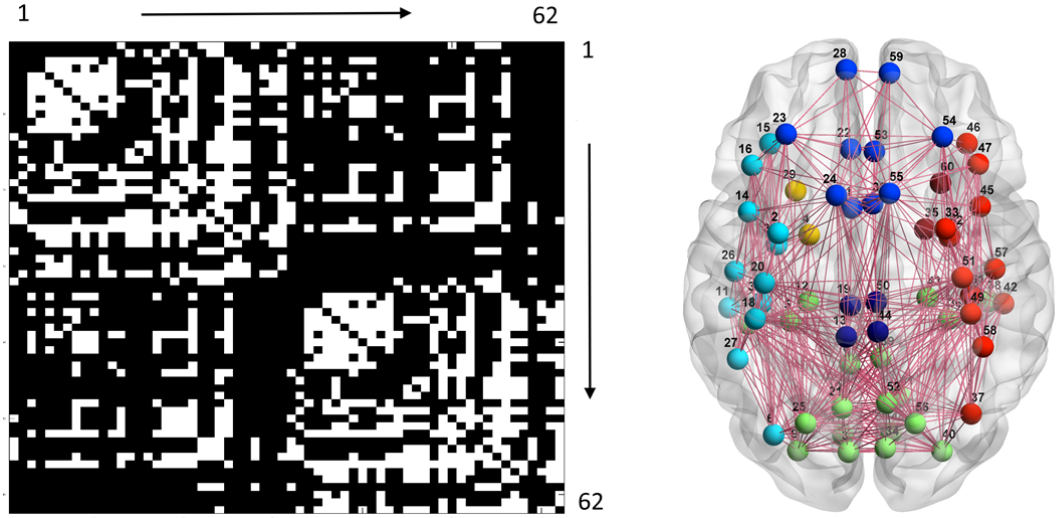

Fig. 2. Left: group-level SC map. Right: results of the associated community detection analysis. Please refer to the legend of Figure 1 for other details.

Brain Connectivity
Revisiting the functional and structural connectivity of large-scale cortical networks (DOI: 10.1089/brain.2017.0536)

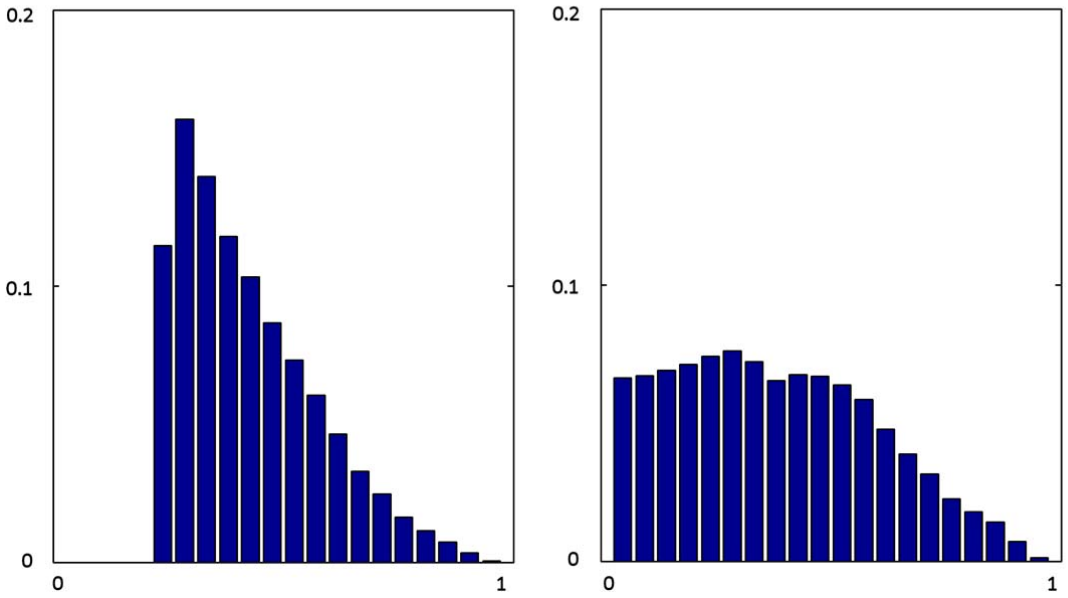

Fig. 3. Histograms of correlation coefficients of BOLD from significant connections in FC (left) and from the connections in SC (right). Ordinate is the probability; abscissa is the correlation level divided into 20 bins, ranging from 0 to 1.

Brain Connectivity
Revisiting the functional and structural connectivity of large-scale cortical networks (DOI: 10.1089/brain.2017.0536)

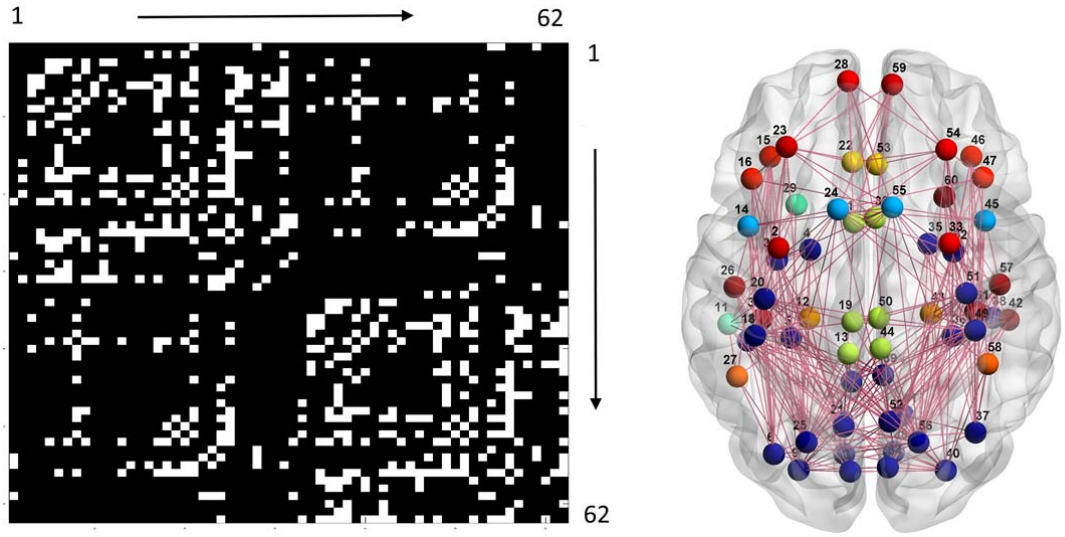

Fig. 4. Left: group-level SC-FC differential map. Right: results of the associated community detection analysis. Please refer to the legend of Figure 1 for other details.

Brain Connectivity
Revisiting the functional and structural connectivity of large-scale cortical networks (DOI: 10.1089/brain.2017.0536)

Supplementary Data

The supplementary information contains three sections: (1) the statistical issue of within-modality cross-subject versus cross-modality within-subject comparison, (2) the illustration of anatomical segmentation (by FreeSurfer) and whole brain deterministic fiber tracking (by FATCAT) for visual assessment of quality, and (3) the results of FC and SC concordance.

Part I

We would like to address a statistical issue raised by an anonymous *Reviewer*. In the comparison of Jaccard indices in within-modality cross-subject condition versus cross-modality within-subject condition, the sampling of the former is not independent. Our original analysis performed an extensive search of all the possible pairs out of the 36 subjects. The pro was that the sampling was unbiased; however, the con was that the sampling may comprise redundant information. For example, the Jaccard index of subject pairs A-B and B-C may contain the information of subject pair B-C. Here, we carried out another set of comparisons to examine whether the conclusion still holds that the dissimilarity of modular organization between SC and FC of the same subject was far greater than that of FC (and SC) across different subjects.

We randomly grouped 36 subjects into 18 pairs, and calculated 18 Jaccard indices of the 18 pairs, with each subject only used once. The 18 data points were then compared with the 36 data points obtained from cross-modality within-subject condition. The above procedure was repeated for 1,000 times, and we can get an idea of the range of statistical difference of the two conditions. Compared with cross-modality within-subject condition (mean 0.17, STD 0.03), the grand mean and mean STD of the 1,000 calculations of cross-subject SC maps were 0.36 and 0.12 with maximum *P* value 10^{-7} and minimum t-score 5.80, while those of cross-subject FC maps were 0.26 and 0.08 with maximum *P* value 10^{-4} and minimum t-score 4.23. Our results showed that different sampling strategies would influence the statistical significance but the conclusion still remains.

Since this article is about SC and FC, we would like to share our personal viewpoint on a terminology that we believe needs to be corrected. In neuroimaging circle, the term

“functional connectivity” is regarded as a contrary to causal connectivity. The semantics of causal, however, is not opposite to functional and causal influence is obviously also functional. Actually, the term FC used to be contrasted with SC (not with causality), which enjoys much longer history in neuroscience (e.g. in the field of neurophysiology) than that limiting FC to bivariate correlation. It seems more appropriate to position the term "functional connectivity" at higher hierarchy, in contrast to SC, so as to accommodate various different kinds of relationship of neural dynamics, such as correlated, Granger, statistically dependent, structural-equation-modelled connectivity, and so on.

Brain Connectivity
Revisiting the functional and structural connectivity of large-scale cortical networks (DOI: 10.1089/brain.2017.0536)
This paper has been peer-reviewed and accepted for publication, but has yet to undergo copyediting and proof correction. The final published version may differ from this proof.

Part II

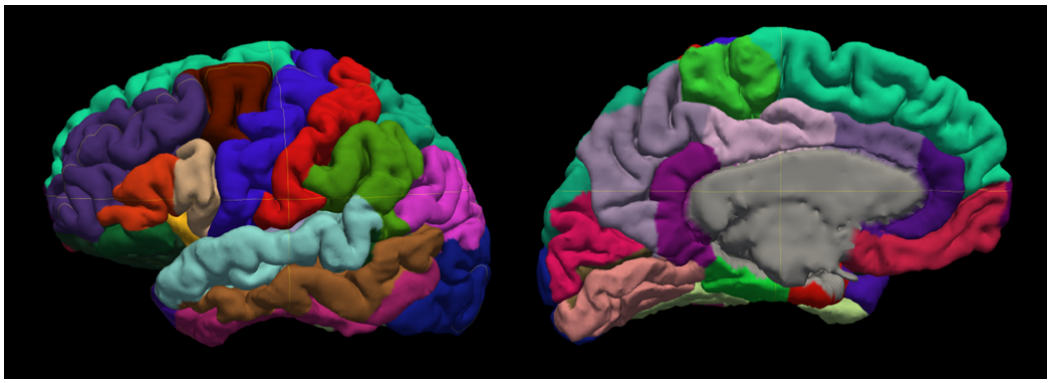

Supp. Figure 1. Exemplar illustration of the cortical parcellation results of FreeSurfer from randomly selected subject. Left and right subplots are lateral and medial views. The extents of different ROIs are delineated by different colors.

Brain Connectivity
Revisiting the functional and structural connectivity of large-scale cortical networks (DOI: 10.1089/brain.2017.0536)

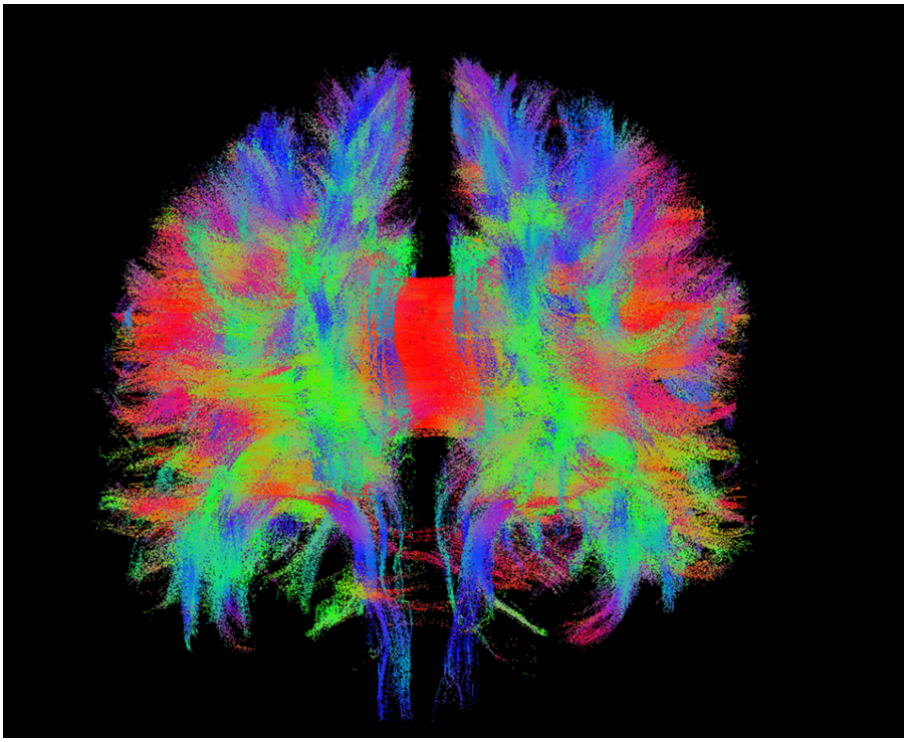

Supp. Figure 2. Exemplar illustration of whole brain tractography by FATCAT from randomly selected subject.

Brain Connectivity
Revisiting the functional and structural connectivity of large-scale cortical networks (DOI: 10.1089/brain.2017.0536)

Brain Connectivity
Revisiting the functional and structural connectivity of large-scale cortical networks (DOI: 10.1089/brain.2017.0536)

Part III

Part III summarizes the connections that are concordant between FC and SC maps. The patterns of FC and SC are both affected by selected thresholds and it is hard to determine what the correspondent thresholds are for FC and SC regarding a systemic exploration (note: this study mainly used modularity analysis to compare FC and SC that is less vulnerable to threshold selection). The results are thus for interested readers' reference only.

Despite the partial mismatch illustrated above, interesting patterns shared by FC and SC maps were also observed. Sensorimotor ROIs in FC and SC are a good example. In addition to classical sensorimotor ROIs (PreCG and PoCG), the secondary sensory cortex (SMG), auditory cortex (TTG) and viscero-motor/-sensory center (INS) were all functionally linked as a neural community. The sensorimotor module of the FC map thus integrates somatic, auditory and visceral functions as a whole to facilitate responses to external and internal environmental challenges. Similarly, the SC sensorimotor ROIs were not isolated but were embedded within a much broader context (the ventral brain module), which also encompassed the TTG, SMG and INS. Regarding the module of the visuo-associative area, both FC and SC maps included occipital, parietal, and inferior temporal regions. We acknowledge that the above inferred neuropsychological functions associated with modular organizations are not immune to the criticism of circular analysis (Kriegeskorte et al., 2009, 2010). Exploration of the relationship between the graph features and neuropsychological performance may provide preliminary hint to the functions of these modules, especially the modules situated at lower FC strengths.

Brain Connectivity
Revisiting the functional and structural connectivity of large-scale cortical networks (DOI: 10.1089/brain.2017.0536)

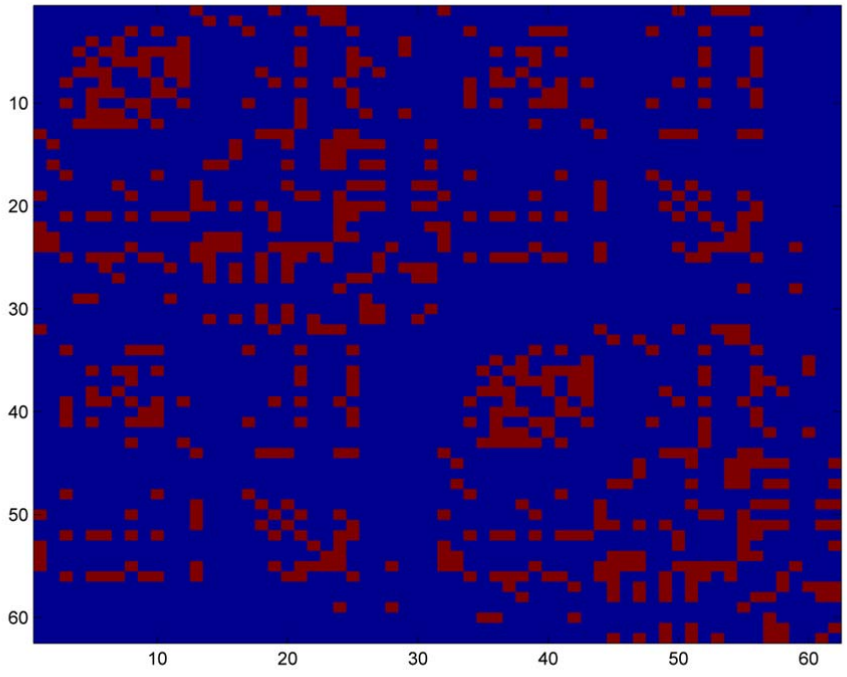

Supp. Figure 3. The concordance between group-level FC and SC maps, presented as a matrix (red: connected, blue: disconnected). The numbers 1-62 in Figures 3-6 represent parcellated cortical brain regions; please refer to Table 1 for detail.

Brain Connectivity
Revisiting the functional and structural connectivity of large-scale cortical networks (DOI: 10.1089/brain.2017.0536)

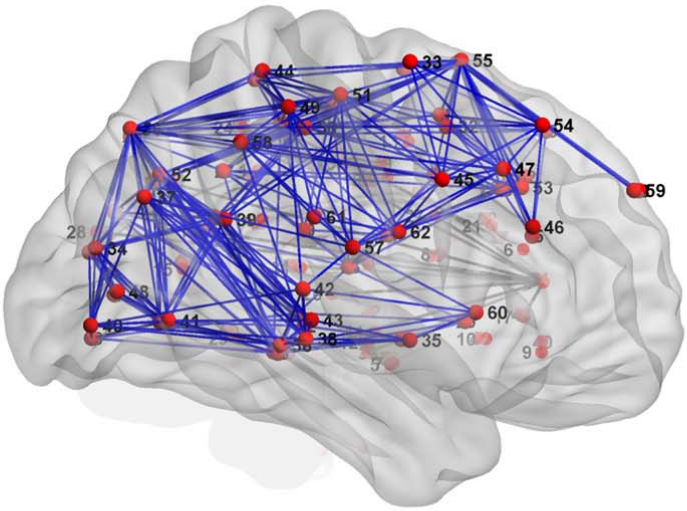

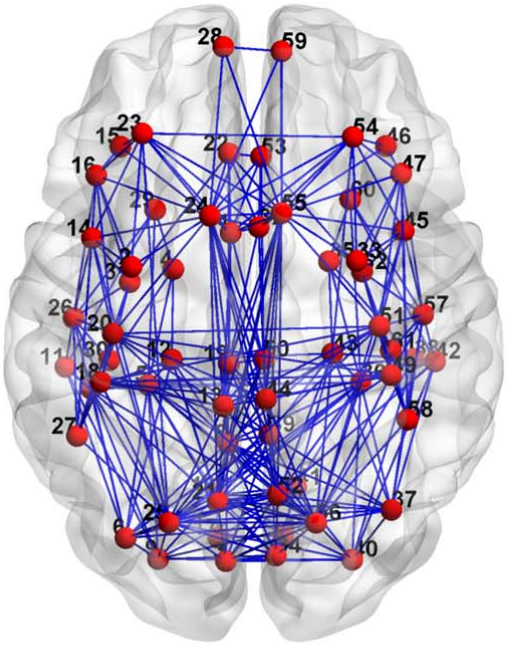

Brain Connectivity
Revisiting the functional and structural connectivity of large-scale cortical networks (DOI: 10.1089/brain.2017.0536)

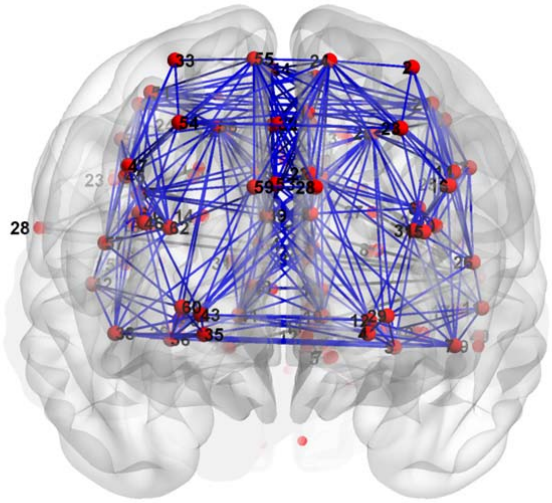

Supp. Figures 4-6. The concordance between group-level FC and SC maps, illustrated by BrainNet Viewer and visualized in sagittal, axial and coronal views.